Transient sum-frequency generation in resonant three-level media

John A. Benda*
Institute of Optics, University of Rochester, Rochester, New York 14627
and Xerox Corporation, Wilson Center for Technology, 800 Phillips Road, Webster, New York 14580

Daniel J. Gauthier and Robert W. Boyd
Institute of Optics, University of Rochester, Rochester, New York 14627
(Received 12 August 1985)

Resonantly enhanced sum-frequency generation of pulsed laser radiation is treated theoretically for the case of a three-level system. The density-matrix equations of motion are solved using second-order, time-dependent perturbation theory with the inclusion of transient effects. The energy and spectrum of the generated radiation are calculated as functions of laser detunings, laser pulse lengths, and temporal overlap of the laser pulses. The tuning characteristics and output pulse characteristics are found to differ qualitatively depending on whether or not the excitation pulses satisfy the adiabatic following criteria generalized for the case of a three-level atom.

INTRODUCTION

Nonlinear optical interactions are typically described in terms of the nonlinear optical susceptibility,[1] which is obtained by calculating the steady-state response of the material system to applied optical fields. However, experiments are often conducted using pulsed lasers, and when the pulse length is comparable to or smaller than the relaxation times of the medium, the steady-state treatment of the nonlinear response must be modified to include transient effects.[2,3] Transient effects in nonlinear optics have been discussed by Grischkowsky[4] and by Courtens and Szoke,[5] primarily for the case of a two-level system, and by Tai[6] for the case of third-harmonic generation. In this paper we present an analysis of resonantly enhanced sum-frequency generation (SFG) involving pulsed lasers, as illustrated in Fig. 1(a). Our analysis is applicable to resonantly enhanced SFG in media such as noncentrosymmetric crystals doped with impurity ions,[7] or atomic vapors in the presence of a symmetry-breaking static electric field.[8] We determine the induced polarization near the sum frequency $\omega_3=\omega_1+\omega_2$ by calculating the Fourier components of the density-matrix element ρ_{ca} oscillating at frequencies near ω_3. We assume that the laser pulses are sufficiently weak that saturation effects[9,10] are unimportant, and hence that it is sufficient to calculate ρ_{ca} using second-order perturbation theory. For certain specific forms for the laser pulse shapes, we derive the form of the output pulse shape, and we present specific predictions for the energy conversion efficiency and output spectrum in terms of the laser frequencies and time delay between the laser pulses.

The theoretical predictions of this paper are found to differ qualitatively, depending on whether or not the excitation obeys the adiabatic following criterion. According to the criterion established by Courtens and Szoke[5] for a two-level system, a laser pulse is nonadiabatic only if its spectrum appreciably overlaps the atomic transition frequency. In this case, population can remain in the upper level at the end of the excitation pulse, leading to an oscillating dipole moment that persists after the excitation has ended. In this paper we generalize the concept of adiabatic following to apply to the excitation scheme shown in Fig. 1. We consider the excitation to be adiabatic [Fig.

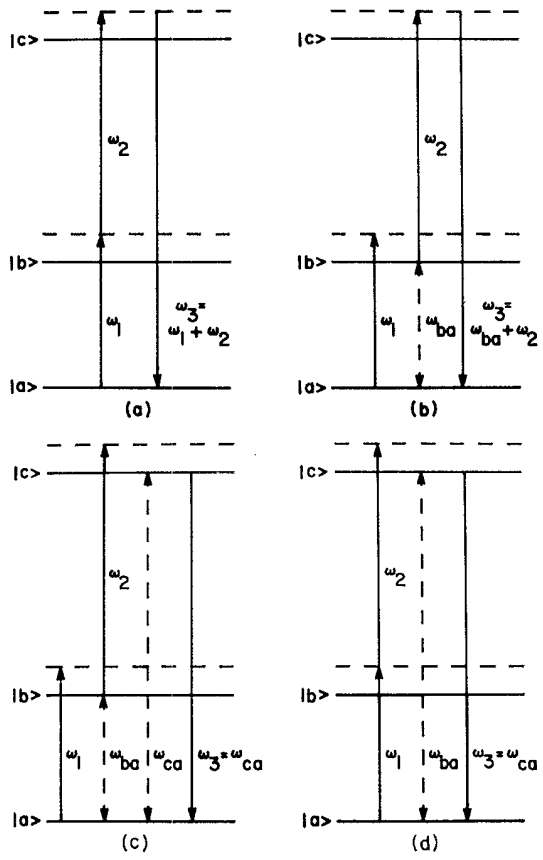

FIG. 1. (a) Sum-frequency generation in a three-level atomic system. (b) If the ω_1 pulse is nonadiabatic, the dipole moment connecting levels a and b can have a component at frequency ω_{ba}, leading to the generation of coherent output at frequency $\omega_3=\omega_{ba}+\omega_2$. (c) and (d) If the excitation of level c is nonadiabatic, coherent output is produced at frequency $\omega_3=\omega_{ca}$.

1(a)] if the one-photon excitation has no frequency components that appreciably overlap the $b \rightarrow a$ transition frequency, and if the two-photon excitation has no frequency components that appreciably overlap the $c \rightarrow a$ transition frequency. As illustrated in Figs. 1(b)–1(d), under nonadiabatic excitation up to three new carrier frequencies can be generated; these new frequencies are ω_{ca} and $\omega_{ba}+\omega_2$, in addition to the sum frequency $\omega_1+\omega_2$. Furthermore, it is found that if the first pulse is nonadiabatic, the total energy of the generated radiation can be maximized by introducing a time delay between the input pulses; this time delay can under extreme conditions be comparable to the length of the pulses. The tuning characteristics of the nonlinear mixing process and time evolution of the output are also found to differ qualitatively, depending on whether or not the excitation is adiabatic.

THEORETICAL DEVELOPMENT

For the three-level system illustrated in Fig. 1, the density-matrix equations of motion take form[11,12]

$$\frac{\partial \rho_{ij}}{\partial t} = -i\omega_{ij}\rho_{ij} - \Gamma_{ij}\rho_{ij} + (i\hbar)^{-1}\sum_{\nu}(\rho_{i\nu}\mu_{\nu j} - \mu_{i\nu}\rho_{\nu j})E(t) \tag{1}$$

for i,j equal to a, b, and c. Here $E(t)$ is the instantaneous value of the electric field, $\hbar\omega_{ij}$ is the energy difference between levels i and j, μ_{ij} is the ij matrix element of the dipole moment operator, and Γ_{ij} is the relaxation rate associated with the element ρ_{ij}. We obtain a perturbative solution to Eq. (1) by expressing ρ_{ij} as

$$\rho_{ij} = \rho_{ij}^{(0)} + \rho_{ij}^{(1)} + \rho_{ij}^{(2)} + \cdots \tag{2}$$

and inserting the nth order solution in the term containing $E(t)$, then solving for the $(n+1)$th order solution. The applied electric field is expressed as

$$\begin{aligned} E(t) &= E_1(t) + E_2(t) \\ &= \tfrac{1}{2}\epsilon_1(t)e^{-i\omega_1 t} + \tfrac{1}{2}\epsilon_2(t)e^{-i\omega_2 t} + \text{c.c.}\,, \end{aligned} \tag{3}$$

where ω_1 is nearly resonant with ω_{ba} and ω_2 is nearly resonant with ω_{cb}. The field amplitudes ϵ_i are taken to be functions of t since the optical fields are assumed to be pulsed. We now introduced the rotating wave approximation, that is, we retain only those driving terms on the right side of Eq. (1) that oscillate approximately at frequency ω_{ij}. The first- and second-order solutions are found to be

$$\rho_{ba}^{(1)}(t) = \frac{\exp(-i\omega_{ba}t - \Gamma_{ab}t)}{2i\hbar} \times \int_{-\infty}^{t} \mu_{ba}\epsilon_1(\tau)\exp(-i\Delta_1\tau + \Gamma_{ab}\tau)d\tau \tag{4a}$$

and

$$\rho_{ca}^{(2)}(t) = \frac{\exp(-i\omega_{ca}t - \Gamma_{ac}t)}{2i\hbar}\int_{-\infty}^{t}\mu_{ca}\epsilon_2(\tau)\exp[-i(\Delta_2-\omega_{ba})\tau + \Gamma_{ac}\tau]\rho_{ba}^{(1)}(\tau)d\tau\,, \tag{4b}$$

where we have introduced the detuning factors $\Delta_1=\omega_1-\omega_{ba}$, $\Delta_2=\omega_2-\omega_{cb}$, and $\Delta_3=\omega_1+\omega_2-\omega_{ca}$. Perturbative solutions for the remaining matrix elements can be calculated analogously, but are not presented here since they do not contribute to the SFG process.

It has been found by Allen *et al.*[13] that many pulsed lasers emit pulses that can be described by the functional form $t^m e^{-kt}$. The parameter m determines the pulse shape, while k determines the pulse length. This pulse shape is particularly convenient in that it allows us to find closed-form expressions for the integrals appearing in Eqs. (4a) and (4b). To allow the possibility of partially non-overlapping pulses, we let t_0 be the time interval by which the onset of the first pulse preceeds that of the second. We thus express the pulse envelopes as

$$\epsilon_1 = \epsilon_{10}(e/m_1)^{m_1}[k_1(t+t_0)]^{m_1}e^{-k_1(t+t_0)} \quad \text{for } t > -t_0\,, \tag{5a}$$

$$\epsilon_2 = \epsilon_{20}(e/m_2)^{m_2}(k_2 t)^{m_2}e^{-k_2 t} \quad \text{for } t > 0\,, \tag{5b}$$

and $\epsilon_{1,2}=0$ otherwise. The normalization constants ensure that ϵ_{10} and ϵ_{20} denote the maximum field of each pulse.

By substituting Eq. (5a) into Eq. (4a), we obtain the only nonzero first-order matrix element:

$$\rho_{ba}^{(1)}(t) = \frac{G_1\mu_{ba}\epsilon_{10}\exp(i\omega_1 t_0)}{Z_1^{m_1+1}}\left\{\exp[(-i\omega_{ba}-\Gamma_{ba})(t+t_0)] - \exp[(-i\omega_1-k_1)(t+t_0)]\sum_{l=0}^{m_1}\frac{[Z_1(t+t_0)]^l}{l!}\right\}, \tag{6}$$

where we have adopted the notation $Z_1=\Delta_1+i(\Gamma_{ab}-k_1)$, $Z_2=\Delta_2+i(\Gamma_{ac}-\Gamma_{ab}-k_2)$, and $Z_3=Z_1+Z_2=\Delta_3+i(\Gamma_{ac}-k_1-k_2)$ and have defined

$$G_i = -\left[\frac{m_i!}{2\hbar}\right]\left[\frac{-iek_1}{m_i}\right]^{m_i}, \quad i=1,2\,. \tag{7}$$

For comparison, we note that the steady-state solution to Eq. (4a) is given by

$$\rho_{ba,ss}^{(1)} = \frac{\mu_{ba}\epsilon_1}{\hbar}\frac{e^{-i\omega_1 t}}{\Delta_1 + i\Gamma_{ab}}\,. \tag{8}$$

There are two terms in the transient result, one oscillating at the transition frequency ω_{ba} and another oscillating at the input frequency ω_1. We shall see below that the component oscillating at ω_{ba} can give rise to frequency components in the sum frequency polarization at $\omega_2+\omega_{ba}$ and ω_{ca}.

Equations (5b) and (6) are now substituted into Eq. (4b), which is then solved to give the second-order response (for non-negative time delay t_0) as

$$\rho_{ca}^{(2)}(t)=G_1G_2\mu_{ba}\mu_{cb}\epsilon_{10}\epsilon_{20}\left[\frac{e^{-k_1t_0}}{Z_1Z_3^{m_1+m_2+1}}\left[\exp(-i\omega_{ca}t-\Gamma_{ac}t)H_{m_1}-\exp[-i(\omega_1+\omega_2)t-(k_1+k_2)t]\sum_{l=0}^{m_1+m_2}H_{m_1+m_2-l}\frac{(iZ_3t)^l}{l!}\right]+\frac{\exp(i\Delta_1t_0-\Gamma_{ab}t_0)}{Z_1^{m_1+1}Z_2^{m_2+1}}\left[\exp(-i\omega_{ca}t-\Gamma_{ac}t)-\exp[-i(\omega_2+\omega_{ba})t-(k_2+\Gamma_{ab})t]\sum_{l=0}^{m_2}\frac{(iZ_2t)^l}{l!}\right]\right], \tag{9}$$

where

$$H_l=\sum_{l=0}^{\min(l,m_1)}\left[\sum_{k=0}^{j}\frac{(iZ_1t_0)^k}{k!}\right]\frac{(m_1+m_2-j)!}{m_2!(m_1-j)!}\left[\frac{Z_3}{Z_1}\right]^j. \tag{10}$$

This result is to be compared with the steady-state solution to Eq. (4b):

$$\rho_{ca,ss}^{(2)}=\mu_{ba}\mu_{cb}\epsilon_1\epsilon_2\frac{e^{-i(\omega_1+\omega_2)t}}{4\hbar^2(\Delta_1+i\Gamma_{ab})(\Delta_3+i\Gamma_{ac})}. \tag{11}$$

There are two terms in Eq. (9). The first term decays with time delay t_0 with the same decay constant k_1 with which the first laser pulse decays with time. It is similar to steady-state SFG in that it is inversely proportional to powers of the complex detuning factors containing Δ_1 and $\Delta_3=\Delta_1+\Delta_2$, but with the linewidths changed from Γ_{ab} to roughly $|k_1-\Gamma_{ab}|$, and from Γ_{ac} to roughly $|k_1+k_2-\Gamma_{ac}|$. This term includes two carrier frequency components, one oscillating at ω_{ca} and another at the steady-state sum frequency $\omega_1+\omega_2$. The second term in Eq. (9) decays with time delay t_0 with the medium relaxation constant Γ_{ab}, and has a different dependence on detunings. It is inversely proportional to powers of the complex detuning factors containing Δ_1 and Δ_2. Again this term is comprised of two carrier frequency components, one at $\omega_2+\omega_{ba}$ and another at ω_{ca}. The $\omega_2+\omega_{ba}$ component persists no longer than $\epsilon_2(t)$ and is damped at the medium relaxation rate Γ_{ab}.

It can be seen from Eq. (9) that SFG at $\omega_1+\omega_2$ occurs only when the pulses overlap. For non-overlapping pulses, the generation is at nearby, partially resonant frequencies. This conclusion is demonstrated numerically in the next section.

Schematically, the processes that lead to Eq. (9) are shown in Fig. 1. The first pulse at ω_1 produces a dipole moment oscillating at ω_{ba}, from transient excitation, as well as the usual steady-state dipole moment at ω_1. The second pulse at ω_2 interacts with the dipole moments at these frequencies to produce dipole moments at ω_{ca} and $\omega_2+\omega_{ba}$ from transient excitation, as well as the usual steady-state dipole moment at $\omega_1+\omega_2$.

RESULTS

In this section we display graphically our formal results given by Eq. (9) for several cases of experimental interest. We assume two identical laser pulses described by Eqs. (5) with $m_1=m_2=4$ and $k_1=k_2=10$ nsec^{-1}, as illustrated in Fig. 2(a). The field envelope of each pulse has a full width at half maximum (FWHM) of 0.5 nsec. The medium relaxation rates Γ_{ab} and Γ_{ca} are chosen to be 1.0 and 0.3 nsec^{-1}, respectively. The detunings Δ_1 and Δ_2 and the time delay t_0 between the pulses are allowed to vary.

By varying Δ_1 and Δ_2, we can choose whether or not the pulses fall within the adiabatic following limit. As mentioned in the Introduction, adiabatic following occurs if the spectral width of the excitation does not overlap the transition frequency. For pulses of the form t^me^{-kt}, the spectral width (FWHM) in angular frequency units is given approximately by $2k[\ln 2/(m+1)]^{1/2}$. Hence the conditions for adiabatic following are $\Delta_1/2\pi \gg 1$ GHz and $(\Delta_1+\Delta_2)/2\pi \gg 1$ GHz for the values used in our numerical calculations.

Figures 2(b) and 2(c) show the time evolution of the amplitude of the induced dipole moment for conditions under which the pulses are ($t_0=0$) and are not ($t_0=1$ nsec) temporally coincident. Since the expectation value of the dipole moment is given by

$$\langle\mu^{(2)}(t)\rangle=\rho_{ca}^{(2)}(t)\mu_{ac}+\text{c.c.}, \tag{12}$$

the amplitude of the induced dipole moment is proportional to $|\rho_{ca}^{(2)}(t)|$. The results shown in Fig. 2 are normalized by $|\rho_{ca,ss}^{(2)}|$, the density-matrix element under steady-state conditions with applied fields of strength ϵ_{10} and ϵ_{20}. The first pulse is detuned by $\Delta_1/2\pi=2$GHz, and hence is intermediate between the adiabatic and nonadiabatic limits. As the detuning of the second pulse is varied from 0.2 to 20 GHz, the excitation of the $b\rightarrow c$ one-photon transition changes from the nonadiabatic to the adiabatic limit.

For both temporal overlap and non-overlap, the polarization is seen to decay to zero at the end of the second pulse if the second pulse is adiabatic. If the second pulse

is nonadiabatic, the polarization rises quickly and decays slowly with the relaxation rate Γ_{ab}, persisting long after the second pulse has ended.

Figure 3 shows how the output energy W depends on the time delay t_0 between the pulses. The output energy is calculated as

$$W=\int_0^\infty P(t)dt\ , \tag{13}$$

where $P(t)$ is the instantaneous power generated by an interaction volume of length L and effective area A_{eff} containing N atoms per unit volume. Assuming perfect phase matching, the instantaneous power is given by

$$P(t)=\frac{2\pi\omega_3^2}{nc}N^2L^2|\mu_{ac}|^2|\rho_{ca}(t)|^2A_{\text{eff}}\ . \tag{14}$$

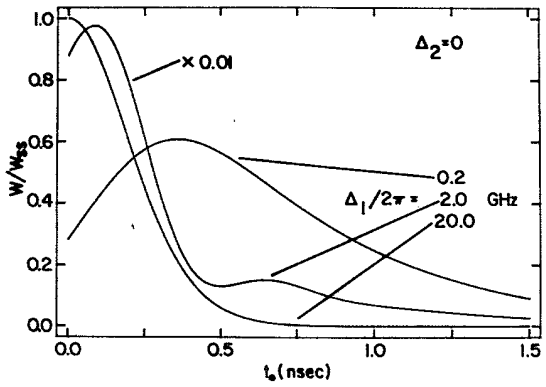

FIG. 3. Output energy vs time delay between the exciting pulses for the case $\Delta_2=0$. The results are normalized by the output pulse energy assuming steady-state response. The case $\Delta_1/2\pi=2.0$ GHz is shown reduced by a factor of 100.

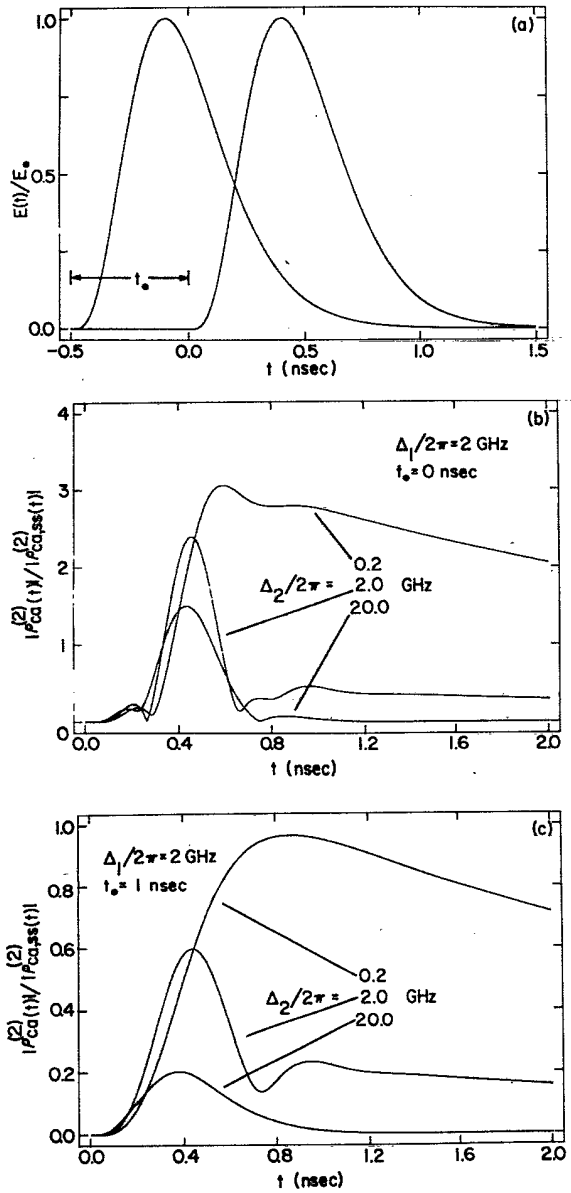

FIG. 2. (a) Time evolution of the two exciting laser pulses shown with a time delay t_0 of 0.5 nsec. (b) and (c) Time evolution of the induced dipole moment producing sum-frequency generation, for a detuning of $\Delta_1/2\pi=2.0$ GHz and the case of (b) temporally coincident pulses and (c) noncoincident pulses.

The ordinate in Fig. 3 has been normalized by the energy W_{ss} predicted by Eqs. (13) and (14) under the assumption that $\rho_{ca}(t)$ is accurately predicted by its steady-state value given by Eq. (11) with ϵ_1 and ϵ_2 given by Eqs. (5) with $t_0=0$.

Figure 3 illustrates the case in which the second laser pulse is tuned to the second resonance ($\Delta_2=0$). For the case in which the first pulse is adiabatic ($\Delta_1/2\pi=20.0$ GHz), the output energy decreased monotonically with time delay and reaches zero when the pulse overlap vanishes. This result is to be expected because ρ_{ba} must equal zero at the end of the first pulse if this pulse is adiabatic (i.e., no population is left in level b), and under these conditions the second pulse cannot excite ρ_{ca}. For the opposite case in which the first pulse is nonadiabatic ($\Delta_1/2\pi=0.2$ GHz), the output energy initially increases with time delay. This result is to be expected because under these conditions a time interval of order Γ_{ab}^{-1} is required before ρ_{ba} attains its maximum value. For longer time delays the energy decreases with t_0 with rate Γ_{ab}.

A plot of the output energy versus the detuning Δ_3 from the two-photon resonance is shown in Fig. 4. Here $\Delta_1/2\pi$ is fixed at 2.0 GHz and the time delay is varied. For time delays less than the pulse length, Eq. (9) predicts that there are two contributions to the excitation spectrum, one centered at the two-photon resonance ($\Delta_3=0$) and another at the second one-photon resonance $\Delta_2=0$ (implying $\Delta_3/2\pi=\Delta_1/2\pi=2.0$ GHz). These two contributions can add either constructively or destructively to give a peak (as in the case of $t_0=0$) or a dip (as in the case $t_0=0.25$ nsec) at intermediate frequencies. When there is no overlap ($t_0=1.0$ nsec), only the one-photon-resonance contribution remains, since ρ_{ba} oscillates at ω_{ba} (and not ω_1) after the end of the first pulse. Under steady-state

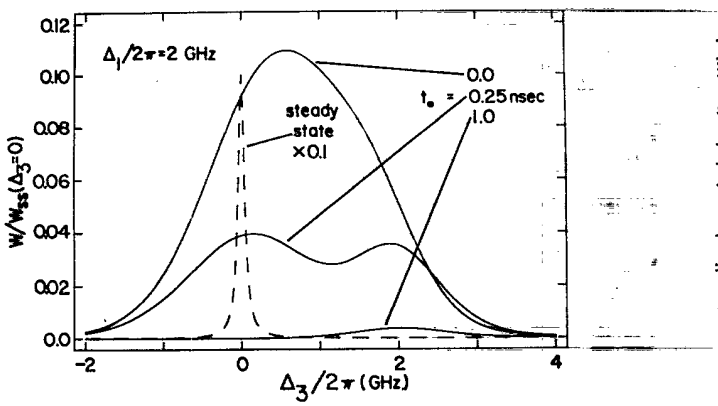

FIG. 4. Output energy vs the detuning Δ_3 from the two-photon resonance, for $\Delta_1/2\pi=2.0$ GHz. The predictions under steady-state conditions are shown for comparison, reduced by a factor of 10. The results are normalized by the maximum value of W_{ss} (at $\Delta_3=0$).

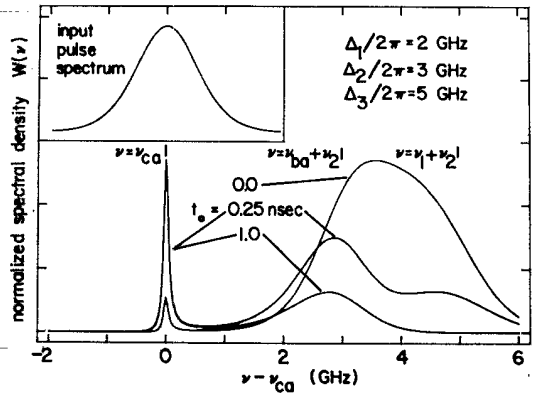

FIG. 5. Spectrum of the generated radiation for several different values of the pulse delay t_0, for $\Delta_1/2\pi=2.0$ GHz, $\Delta_2/2\pi=3.0$ GHz, and $\Delta_3/2\pi=5.0$ GHz. Each curve has been normalized such that its maximum value is unity. The inset shows the spectrum of the input pulses.

conditions, Eq. (14) predicts a detuning curve with a single, narrow peak at the two-photon resonance, as shown (not to scale) in Fig. 5.

The spectral composition of the output $W(\omega)$ is proportional to the square modulus of the Fourier transform of P, and hence to

$$W(\omega)\propto N^2|\mu_{ac}|^2\left|\int_{-\infty}^{+\infty}\rho_{ca}^{(2)}e^{i\omega t}dt\right|^2. \tag{15}$$

By substitution from Eq. (9), we arrive at the following expression for $W(\omega)$:

$$W(\omega)\propto\left|G_1G_2\mu_{ba}\mu_{cb}\epsilon_{10}\epsilon_{20}\left[\frac{\exp(-k_1t_0)}{Z_1Z_3^{m_1+m_2+1}}\left[\frac{H_{m_1}}{i(\omega-\omega_{ca})-\Gamma_{ac}}-\sum_{l=0}^{m_1+m_2}\frac{H_{m_1+m_2-l}(iZ_3)^l}{[i(\omega-\omega_1-\omega_2)-(k_1+k_2)]^{l+1}}\right]\right.\right.$$
$$\left.\left.+\frac{\exp(i\Delta_1t_0-\Gamma_{ab}t_0)}{Z_1^{m_1+1}Z_2^{m_2+1}}\left[\frac{1}{i(\omega-\omega_{ca})-\Gamma_{ac}}-\sum_{l=0}^{m_2}\frac{(iZ_2)^l}{[i(\omega-\omega_2-\omega_{ba})-(k_2+\Gamma_{ab})]^{l+1}}\right]\right]\right|^2. \tag{16}$$

The spectral density of a typical output pulse is illustrated in Fig. 5 for three values of the time delay. All curves have been normalized so that their maxima have the same value. Consistent with Eq. (16), there are three contributions to $W(\omega)$, one centered at the two-photon transition frequency ω_{ca}, one centered at the sum frequency $\omega_1+\omega_2$, and one centered at $\omega_2+\omega_{ba}$. For small time delays, all three are important. The latter two contributions can add constructively or destructively to give either a peak or a dip between $\omega_2+\omega_{ba}$ and $\omega_1+\omega_2$. As overlap between the pulses disappears ($t_0=1.0$ nsec), the sum-frequency peak disappears and the two-photon transition peak increases in importance. Under steady-state conditions, the output spectrum would be simply a delta function at $\omega_1+\omega_2$.

It should be noted that the results presented in this article obey a simple scaling law. If all detunings and relaxation rates are increased by some multiplicative factor and all time variables (pulse width and time delay) are reduced by the same factor, the predictions remain unchanged. Thus, even though the effects of inhomogeneous broadening have not explicitly been included in this calculation, it is expected that the results presented here would remain qualitatively unchanged for the case of laser pulses sufficiently short that their spectral widths exceed the inhomogeneous linewidth.

Also, it should be noted that many of the calculations presented here have been repeated for different values of the pulse-shape parameter, m_1 and m_2, and for Gaussian pulse shapes. No qualitative changes were observed in the

theoretical predictions, and thus we believe that our conclusions are of a rather general nature and are not sensitive to the particulars of the laser pulse shape.

SUMMARY

In summary, we have presented a perturbative, density-matrix calculation of the nonlinear polarization giving rise to transient sum-frequency generation in a resonant, three-level medium. For the case in which the excitation pulses satisfy the adiabatic following criteria, we find that the process is resonantly enhanced only at $\omega_1=\omega_{ba}$ and $\omega_1+\omega_2=\omega_{ca}$, that the output spectrum is peaked at $\omega_1+\omega_2$, that the output pulse length is of the order of the length of the temporal overlap of the two exciting pulses, and that the output energy is maximized by making the pulses temporally coincident. These conclusions are qualitatively similar to those predicted under steady-state conditions as would apply with the use of cw lasers. However, we find that for the opposite case in which the excitation is nonadiabatic, qualitatively different behavior is predicted. In particular, the excitation shows resonances for $\omega_1=\omega_{ba}$, $\omega_1+\omega_2=\omega_{ca}$, and for $\omega_1=\omega_{ba}$, $\omega_2=\omega_{cb}$; the output spectrum shows peaks at $\omega_1+\omega_2$, at $\omega_{ba}+\omega_2$, and at ω_{ca}; the output pulse length is of the order of $1/\Gamma_{ca}$; and the output energy is maximized by introducing a nonzero time delay (of order $1/\Gamma_{ab}$, π/Δ_1, or the pulse length of the first laser, whichever is shorter) between the exciting pulses.

ACKNOWLEDGMENTS

We gratefully acknowledge discussion with M. G. Raymer and C. R. Stroud and research support through the National Science Foundation (Grant No. ECS-8408370) and the Joint Services Optics Program.

---

*Present address: United Technologies Research Center, Silver Lane, East Hartford, CT 06109.

[1]J. A. Armstrong, N. Bloembergen, J. Ducuing, and P. S. Pershan, Phys. Rev. **127**, 1918 (1962).

[2]R. G. Brewer and R. L. Shoemaker, Phys. Rev. Lett. **27**, 959 (1976).

[3]L. Allen and J. H. Eberly, *Optical Resonance and Two-Level Atoms* (Wiley, New York, 1975).

[4]D. Grischkowsky, Phys. Rev. Lett. **24**, 866 (1970).

[5]E. Courtens and A. Szoke, Phys. Rev. A **15**, 1588 (1977).

[6]C. Tai, Phys. Rev. A **23**, 2462 (1981).

[7]K. S. Yngvesson and E. L. Kollberg, Appl. Phys. Lett. **36**, 104 (1980).

[8]D. J. Gauthier, J. Krasinski, and R. W. Boyd, Opt. Lett. **8**, 211 (1983).

[9]R. W. Boyd, M. G. Raymer, P. Narum, and D. J. Harter, Phys. Rev. A **24**, 411 (1981).

[10]T. A. DeTemple, L. A. Bahler, and J. Osmundsen, Phys. Rev. A **24**, 1950 (1981).

[11]L. Allen and C. R. Stroud, Jr., Phys. Rep. **91**, (1982).

[12]D. Marcuse, *Principles of Quantum Electronics* (Academic, New York, 1980).

[13]L. Allen, K. A. Eagles, and C. R. Stroud, Jr., J. Phys. B **15**, 1643 (1982).